phys. stat. sol. (b) **244**, No. 12, 4542–4545 (2007) / **DOI** 10.1002/pssb.200777399

Effects of A-site ionic size variation on the magnetic and transport properties of $(Pr_xSm_{1-x})_{2/3}Sr_{1/3}MnO_3$ ($0 \le x \le 1$)

Saket Asthana[1,2], **Joonghoe Dho**[*,1], and **D. Bahadur**[2]

[1] Department of Physics, Kyungpook National University, Daegu 702-701, Korea
[2] Department of Metallurgical Engineering and Materials Science, Indian Institute of Technology, Bombay 400076, India

Received 30 April 2007, revised 5 October 2007, accepted 20 October 2007
Published online 12 December 2007

PACS 61.10.Nz, 61.66.Dk, 71.38.+k, 75.47.Lx

The effects of average A-site ionic size on magnetic and transport properties have been studied in $(Pr_xSm_{1-x})_{2/3}Sr_{1/3}MnO_3$ ($0 \le x \le 1$) manganites with fixed carrier concentration. An effect of average A-site ionic radius ($\langle r_A \rangle$) with the Pr substitution has been clearly observed in the continuous changes of ferromagnetic transition temperature and metal–insulator transition temperature. The change of the resistivity with the *x* was explained by a variation in the hopping integral between Mn^{3+} and Mn^{4+}, which is dependent on the Mn-O-Mn bond angle affected by the average A-site ionic size. Remarkably, the Sm-doped manganites showed an antiferromagnetic transition by the rare-earth moments below 50 K as well as the ferromagnetic transition by Mn moments at a higher temperature. A phase diagram of $(Pr_xSm_{1-x})_{2/3}Sr_{1/3}MnO_3$ ($0 \le x \le 1$) was successfully constructed on the basis of magnetic and transport studies.

1 Introduction

The physical properties of the substituted manganites are basically explained by the double exchange (DE) interaction associated with electron hopping from Mn^{3+} to Mn^{4+} [1]. The DE interaction, which favors ferromagnetic (FM) and metallic behavior, competes with the Jahn-Teller (JT) effect which favors antiferromagnetic (AFM) and insulating behavior. Recent studies have shown that DE alone cannot explain various physical properties of manganites [2] and other effects such as charge ordering, average A-site cationic radius $\langle r_A \rangle$, A-size cationic size mismatch [3, 4], etc. also play important roles. The average size of the A-site cation of substituted manganites and thus the size mismatch at the A-site modify the Mn-O-Mn bond angle and affect the e_g electron hopping between Mn^{3+} and Mn^{4+}. A lot of work has been done on substituted manganites with a single rare earth ion at the A-site [5] but relatively few reports are on the effect of two rare-earth ions [6, 7].

2 Experimental details

The polycrystalline manganites $(Pr_xSm_{1-x})_{2/3}Sr_{1/3}MnO_3$ (x = 0, 1/6, 2/6, 3/6, 4/6, 5/6, 1) were synthesized by the chemical citrate-gel route using high purity Pr_6O_{11}, Sm_2O_3, $SrCO_3$ and Mn-acetate. The as-prepared powders were calcined at 1000 °C for two hours in air. The powders were pelletized and sintered at 1200 °C for two hours in air. X-ray diffraction (XRD) data were collected using Cu-Kα radiation

* Corresponding author: e-mail: jhdho@knu.ac.kr

(PW 3040/60 Philips, PANalytical) and the resistivity was measured using the standard four-probe dc method from 300 K to 25 K. Magnetic measurements were performed on Quantum design MPMS system upon heating after zero-field-cooling with the rate of 8 K/min.

3 Results and discussion

The XRD patterns for $(Pr_xSm_{1-x})_{2/3}Sr_{1/3}MnO_3$ ($0 \le x \le 1$) compositions revealed that all samples are single phase of an orthorhombic structure. The average A-site ionic radius $<r_A>$ increases with the increase of the Pr content because of a larger ionic size of Pr ion (1.29 Å) in comparison with the Sm ion (1.24 Å). The $<r_A>$ increases from 1.307Å for $x = 0$ to 1.34 Å for $x = 1$ while the A-site size variance decreases from 0.009 $Å^2$ for $x = 0$ to 0.005 $Å^2$ for $x = 1$. This is due to an ionic size difference between Pr^{3+}/ Sm^{3+} and Sr^{2+} (1.44 Å) ions (here, the mean radius is based on the twelve coordination number) [8].

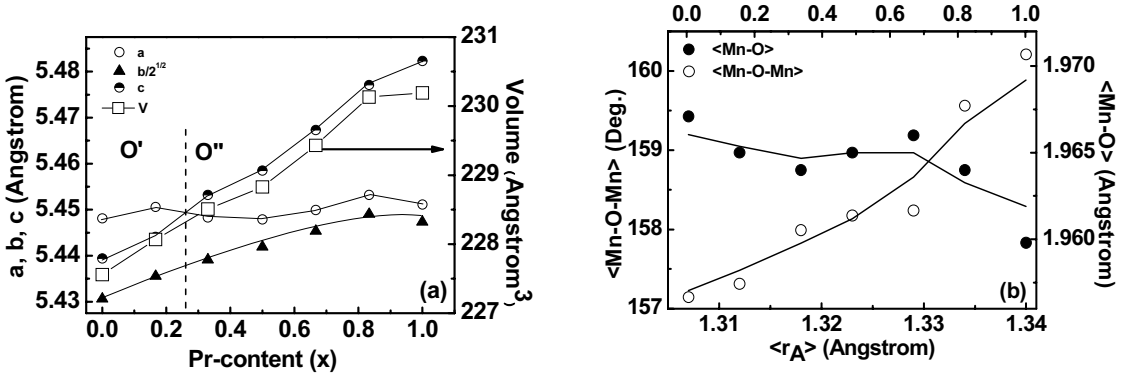

Fig. 1 a) Lattice parameters and unit cell volume for varying Pr content of $(Pr_xSm_{1-x})_{2/3}Sr_{1/3}MnO_3$ and b) average bound angle and bond distance for varying A-site ionic radius.

The structural parameters of these compounds were analyzed by the Rietveld refinement for the XRD data. Figure 1 shows the refined lattice parameters and the unit cell volume with the Pr content. The two different types of orthorhombic structures (O′ ($a > c > b/\sqrt{2}$) and O″ ($c > a > b/\sqrt{2}$)) are clearly observed below and above $x \approx 0.3$, as shown in Fig. 1a. The lattice parameters "c" and "b" increase gradually while the parameter "a" shows only a small variation with increasing the Pr content. The variations of average bond angle (<Mn-O-Mn>) and bond distance (<Mn-O>) are shown in the Fig. 1b. Interestingly, the Mn-O-Mn bond angle increases with the Pr substitution while the Mn-O bond distance slightly decreases. These results should be due to the larger ionic size of Pr^{3+} (1.29 Å) than Sm^{3+} (1.24 Å) and it shows that the A-site ionic size and the size variance clearly affect on the lattice distortion. We guess that the MnO_6 octahedron becomes symmetric as the $<r_A>$ approaches to the O^{2-} ionic size (1.40 Å).

Figures 2a and b show the zero-field cooled (ZFC) and field cooled (FC) magnetization (M) as a function of the temperature in 100 Oe field. The ferromagnetic transition temperature (T_C) gradually increases with the increase of the $<r_A>$. The variation in the T_C with the $<r_A>$ is consistent with the established phase diagram by Hwang et al. [9]. The observed FM transition above 100 K should be due to an alignment of the Mn moments. On the other hand, the rare-earth magnetic moments of Sm^{3+} and/or Pr^{3+} can also display another magnetic transition, which may be a FM or AFM ordering with respect to the ordered Mn moments. In the ZFC magnetization, the AFM transition feature is observed in all the samples except $x = 1$. That is to say, the samples with $x < 5/6$ show an AFM transition behavior by the rare earth magnetic moments below 50 K. The AFM transition temperature (T_N) shifts to a lower temperature with increasing the Pr content. The presence of the rare-earth magnetic moments was supported by the fact that the saturation magnetization value of the Pr-doped samples in 5 T field varies from 3.81 to 3.97 μ_B/f.u. with increasing the x, which is larger than the theoretical value of 3.7 μ_B/f.u.. The observed

magnetic transition data implies that the Sm^{3+} magnetic moments tend to align antiferro-magnetically with the Mn-sublattice while the Pr^{3+} magnetic moments are ordered ferromagnetically.

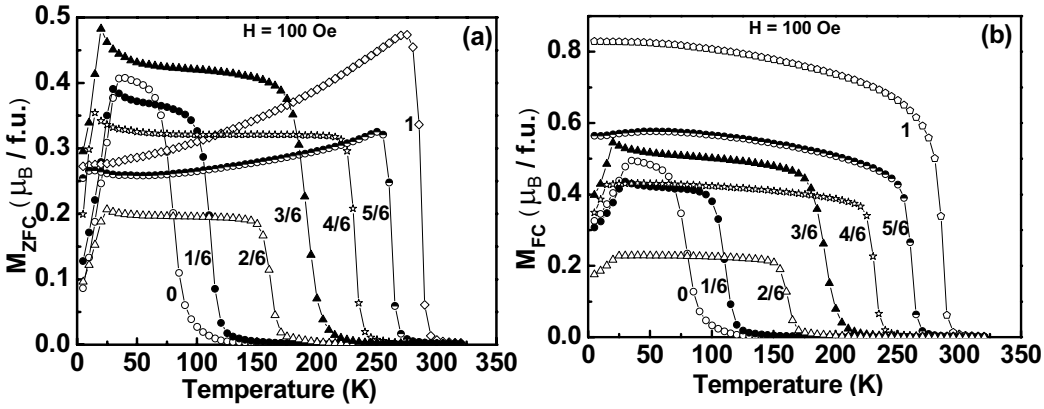

Fig. 2 Temperature dependence of magnetization for $(Pr_xSm_{1-x})_{2/3}Sr_{1/3}MnO_3$ ($0 \le x \le 1$) in (a) ZFC and (b) FC runs. Magnetization was measured in 100 Oe upon warming.

Figure 3 shows the temperature dependence of resistivity for $(Pr_xSm_{1-x})_{2/3}Sr_{1/3}MnO_3$ and the inset shows the variation of resistivity at 25 K and at T_{MI} as a function of $\langle r_A \rangle$, displaying that the resistivity gradually decreases with increasing the $\langle r_A \rangle$. The metal-insulator transition (T_{MI}) shifts to a higher temperature with increasing the Pr^{3+} content. This may be due to the suppression of ionic size variance which is induced by replacing the smaller size Sm^{3+} ion with a larger size Pr^{3+} ion. The magnitude of resistivity above T_{MI} increases marginally with decreasing $\langle r_A \rangle$, but the temperature dependence of resistivity is very similar for all the samples. This implies that the nature of the conduction mechanism above T_{MI} is basically same and the change of resistivity with x simply reflects a variation in the hopping integral between the adjacent Mn^{3+} and Mn^{4+} sites. The hopping integral should be critically affected by the Mn-O-Mn bond angle closely related to the average A-site ionic size effect (see Fig. 1b). The increase of the $\langle r_A \rangle$ from 1.307 Å (x = 0) to 1.34 Å (x = 1) leads to a decrease in the distortion of the MnO_6 octahedron. Theoretically, the electron hopping between Mn^{3+} and Mn^{4+} sites is determined by Mn-O-Mn bond angle. The transfer integral is typically defined as $t = t_0 cos(\theta/2)$, where t_0 is a constant value for the parallel spin arrangement and θ is the angle between the core spins [10]. The transfer integral increases as the Mn-O-Mn angle approaches to 180°, and thus it facilitates the double exchange (DE) interaction leading to the decrease of resistivity. As seen in Fig.1, an average <Mn-O-Mn> bond angle increases from 155.7° (for x = 0) to 160.2° (for x =1) while the <Mn-O> slightly decreases with the Pr content. Therefore, we conjecture that the increase of the hopping integral with increasing x leads to a decrement of the resistivity and a shift of the T_{MI} from 90 K for x =0 to 280 K for x = 1. In our samples, the conduction mechanism can be understood by the small polaron hopping model as discussed in our previous report [11].

Above results indicate that the most paramount parameter determining the physical properties for a fixed carrier concentration is presumably the A-site average ionic size $\langle r_A \rangle$ (or the size variance σ^2_A). Figure 4 shows a phase diagram of $(Pr_xSm_{1-x})_{2/3}Sr_{1/3}MnO_3$ which has been developed through the current magnetic and transport studies. Inset shows the variation of T_{MI} with the σ^2_A and follows the linear variation as discussed in Ref. [4]. Three different regions of PM-I, FM-M and AFM-M are delineated in the phase diagram. The high temperature FM-M phase boundary is due to the Mn moments while the low temperature AFM-M phase boundary is due to the rare-earth moments. As the Pr content increases, the AFM ordering behavior gradually disappears.

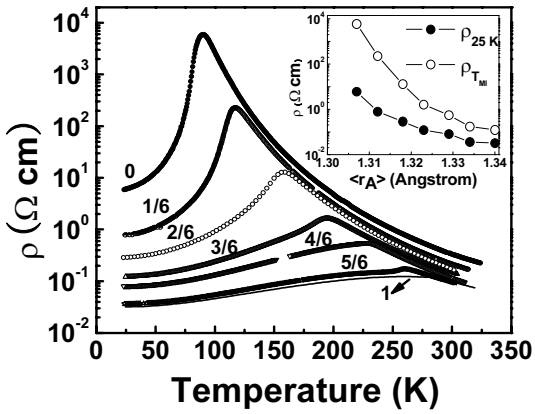

Fig. 3 Temperature dependence of resistivity for $(Pr_xSm_{1-x})_{2/3}Sr_{1/3}MnO_3$ ($0 \le x \le 1$). Inset shows resistivities at 25 K and at T_{MI} as a function of $<r_A>$.

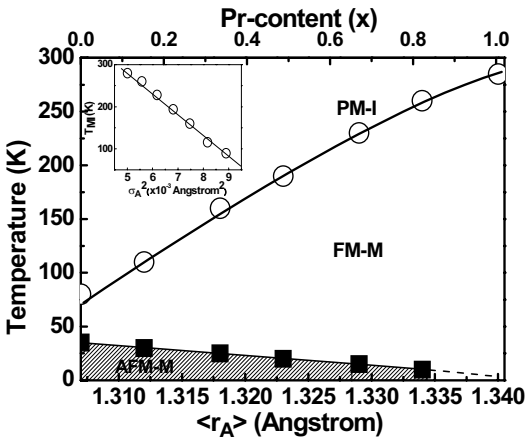

Fig. 4 A phase diagram of $(Pr_xSm_{1-x})_{2/3}Sr_{1/3}MnO_3$. Inset shows the variation of T_{MI} with A-site size variance.

4 Conclusions

The magnetic and transport properties of the series $(Pr_xSm_{1-x})_{2/3}Sr_{1/3}MnO_3$ ($0 \le x \le 1$) have been studied. All systems are crystallized in two types of orthorhombic structure (O′ ($a > c > b/\sqrt{2}$) and O″ ($c > a > b/\sqrt{2}$)) with varying the Pr content. In our samples, the transition temperatures T_{MI} and T_C showed a nearly linear dependence with *x*. Interestingly, our samples displayed AFM transition behavior below 50 K in addition to the FM transition by the Mn moments above 100 K. It seems that the Sm^{3+} spins tend to align antiferro-magnetically with the Mn-sublattice while the Pr^{3+} spins presumably ordered ferromagnetically. The physical properties of our samples with a fixed carrier concentration were well explained by the variation of the $<r_A>$ and the σ^2_A with the *x*.

Acknowledgements The authors Saket Asthana and D.Bahadur, are thankful to the Department of Science and Technology, India for support of the project. This work was partly supported by the BK21 research program and the Korea Research Foundation Grant (Basic Research Promotion Fund, KRF-2006-C00536).

References

[1] S. Jin, T. H. Tiefel, M. Mc Cormack, R. A. Fastnacht, R. Ramesh, and L. H. Chen, Science **264**, 413 (1994).
[2] A. J. Millis, P. B. Littlewood, and B. I. Shraiman, Phys. Rev. Lett. **74**, 5144 (1995).
[3] S. Asthana, A. K. Nigam, and D. Bahadur, phys. stat. sol. (b) **243**, 1922 (2006).
[4] L. M. Rodriguez-Martinez and J. P. Attfield, Phys. Rev. B **54**, 15622 (1996).
[5] C. N. R. Rao and B. Raveau, Colossal Magnetoresistance, Charge Ordering and Related Properties of Manganese Oxides (World Scientific, Singapore, 1998).
[6] W. J. Li, B. Zhang, and W. Lu, Solid State Commun. **140**, 503 (2006).
[7] G. Venkataiah, V. Prasad, and P. V. Reddy, Solid State Commun. **140**, 73 (2007).
[8] R. D. Shannon, Acta Crystallogr. A **32**, 751(1976).
[9] H. Y. Hwang, S. W. Cheong, P. G. Radaelli, M. Marezio, and B. Batlogg, Phys. Rev. Lett. **75**, 914 (1995).
[10] E. L.Nagaev, Phys. Reports **346**, 387 (2001).
[11] S. Asthana, D. Bahadur, and C. M. Srivastava, Physica B **371**, 241 (2006).

